Available online at www.sciencedirect.com
SCIENCE DIRECT
Catalysis Today 105 (2005) 529–536
CATALYSIS TODAY
www.elsevier.com/locate/cattod

Modelling of an SCR catalytic converter for diesel exhaust after treatment: Dynamic effects at low temperature

Enrico Tronconi [a], Isabella Nova [a,*], Cristian Ciardelli [a], Daniel Chatterjee [b], Brigitte Bandl-Konrad [b], Thomas Burkhardt [b]

[a] *Dipartimento di Chimica, Materiali e Ingegneria Chimica "G. Natta", Politecnico di Milano, P.zza L. Da Vinci 32, 20133 Milano, Italy*
[b] *DaimlerChrysler AG Abteilung RBP/C, HPC: 096-E220, D-70546 Stuttgart, Germany*

Available online 11 July 2005

Abstract

As part of a fundamental and applied work on the development of an unsteady mathematical model of the NH_3-selective catalytic reduction (SCR) process for design and control of integrated after-treatment systems of heavy-duty engines, we present herein a transient kinetic analysis of the standard SCR NO + NH_3 system which provides new insight in the catalytic kinetics and mechanism prevailing at low temperatures. Based on kinetic runs performed over a commercial powdered V_2O_5–WO_3–TiO_2 catalyst in the 175–450 °C *T*-range feeding NH_3 and NO (1000 ppm) in the presence of H_2O (1–10%, v/v) and O_2 (2–6%, v/v), an original dual-site modified redox rate law is derived which effectively accounts for NH_3 inhibition effects observed during transient reactive experiments at $T < 250$ °C. We also demonstrate that implementation of the novel modified redox kinetics into a fully predictive 1D + 1D model of SCR monolith reactors can significantly improve simulations of SCR transient runs at different scales, including engine test bench experiments over full-scale SCR honeycomb catalysts.

Keywords: SCR; Monoliths; Transient kinetics

1. Introduction

The selective catalytic reduction (SCR) using urea as reducing agent is currently regarded in Europe as the after-treatment technology of choice for heavy-duty diesel vehicles [1], as they have to meet more and more stringent emission standards for both NO_x and particulate matter.

Extensive work is being currently devoted by the motor industry to adapt the well-known SCR process for deNOxing of stack gases from power stations [2] to the specific demands of mobile applications. For example, mobile applications rely on the use of urea as a non-toxic reducing agent, which is hydrolyzed on-board to give ammonia. Other main issues for mobile applications are the operation under strongly transient conditions and the need for enlarging the temperature window of the reaction, particularly towards lower temperatures; this can be accomplished by cofeeding NO_2 (obtained from partial conversion of NO on a pre-oxidizing catalyst) to the SCR catalyst, thus allowing the occurrence also of the so-called *fast* SCR reaction [3], which involves an equimolar stoichiometric mixture of NO and NO_2 reacting with NH_3.

This paper illustrates part of a fundamental and applied research for the development of an unsteady mathematical model of the NH_3-SCR process applicable to design and control of integrated after-treatment systems for vehicles. Herein, we present the development of a model suitable to predict the transient behaviour of the NH_3–NO/O_2 reacting system. This represents the basis for extension to the complete NH_3–NO–NO_2/O_2 reacting system, currently in progress. Nevertheless, it is worth of note that such a model is suitable for analyzing urea-SCR after-treatment devices

* Corresponding author. Tel.: +39 02 2399 3228; fax: +39 02 7063 8173.
E-mail address: isabella.nova@polimi.it (I. Nova).

0920-5861/$ – see front matter © 2005 Elsevier B.V. All rights reserved.
doi:10.1016/j.cattod.2005.06.043

Nomenclature

C_i	gas-phase concentration of species i (mol/m^3 gas)
C_i^{w}	concentration of species i at gas–solid interface (mol/m^3 gas)
C_i^*	intraporous concentration of species i (mol/m^3 gas)
C_{p}	gas specific heat (J/(kg K))
$C_{\mathrm{p,s}}$	solid phase specific heat (J/(kg K))
d_{h}	hydraulic diameter of monolith channel (m)
$D_{\mathrm{eff},i}$	effective intraporous diffusivity of species i (m^2/s)
E_{des}°	activation energy for NH_3 desorption at zero-coverage (J/mol)
E_{NO}	activation energy for the DeNOx reaction (J/mol)
E_{ox}	activation energy for NH_3 oxidation (J/mol)
h	gas–solid heat transfer coefficient (W/(m^2 K))
$\Delta H_{\mathrm{f},i}$	enthalpy of formation of species i (J/mol)
k_{ads}	rate constant for NH_3 adsorption (s^{-1})
k_{des}°	pre-exponential factor for NH_3 desorption rate constant (mol/(m^3 s))
k_{mt}	mass transfer coefficient (m/s)
k_{NO}°	pre-exponential factor for DeNOx reaction rate constant (s^{-1})
k_{ox}°	pre-exponential factor for NH_3 oxidation rate constant (mol/(m^3/s))
K_i	rate parameter
L	monolith length (m)
R	ideal gas constant (J/(mol K))
$R_{\mathrm{eff},i}$	effective surface rate of formation of species i (mol/(m^2 s))
R_i	intrinsic volumetric rate of formation of species i (mol/(m^3 s))
$r_{\mathrm{NH_3}}$	net rate of NH_3 adsorption (mol/(m^3 s))
r_{NO}	rate of DeNOx reaction (mol/(m^3 s))
r_{ox}	rate of NH_3 oxidation (mol/(m^3 s))
$p_{\mathrm{O_2}}$	oxygen partial pressure (atm)
S_{w}	half-thickness of monolith wall (m)
t	time (s)
T	temperature (K)
T_{g}	gas temperature (K)
T_{s}	catalyst temperature (K)
v	gas linear velocity (m/s)
x	dimensionless intraporous coordinate
z	dimensionless reactor axial coordinate

Greek letters

β	O_2 kinetic order in Eqs. (12) and (15)
γ	parameter for surface coverage dependence
θ_i	surface coverage of species i on site 2
ρ_{g}	gas density (kg/m^3)
ρ_{s}	catalyst density (kg/m^3)
σ_i	surface coverage of species i on site 1
$\Omega_{\mathrm{NH_3}}$	catalyst NH_3 adsorption capacity (mol/m^3 cat)

for heavy-duty applications without pre-oxidizing catalyst, hence based on the $NH_3 - NO/O_2$ reaction only that are compliant with Euro IV/Euro V emission standards and are presently being commercialised.

A stage-wise scale-up approach has been adopted for this project: (i) transient kinetic experiments were performed in a microreactor over an extruded V_2O_5-WO_3/TiO_2 commercial catalyst in powder form (160 mg) in order to evaluate the intrinsic DeNOx kinetics; (ii) such rate expressions, as well as the relevant geometrical and morphological characteristics of the monolith commercial catalyst, were then incorporated into a fully transient heterogeneous 1D + 1D mathematical model of SCR monolith reactors [4], which was first validated against transient SCR runs performed over an honeycomb catalyst sample (up to 10 cm^3) in a laboratory rig; (iii) the final validation was based on extensive test bench data collected in full-scale SCR monolith reactors loaded with catalysts up to 43 l in size, using real diesel engine exhaust gases.

In this paper, the kinetic analysis of the standard SCR NO + NH_3 system, already presented in [5,6] in preliminary form, is extended to gain more fundamental insight into the catalytic kinetics and mechanism prevailing in the low temperature region, which is especially interesting for mobile applications. In particular, previous transient reactive experiments had shown that a decrease of the ammonia gas-phase concentration temporarily enhanced the NO conversion, thus suggesting an inhibiting effect of ammonia that could play a non-negligible role in the SCR reaction [7]. Herein, we derive an original unsteady SCR kinetic model based on a dual-site redox rate expression, and show that such a rate law effectively accounts for the observed NH_3 inhibition effects. We also demonstrate that implementation of the novel kinetics into a fully predictive model of SCR monolith reactors greatly improves simulations of transient runs in engine test bench experiments over full-scale SCR honeycomb catalysts.

2. Experimental

The experiments herein discussed were performed over samples of a single commercial extruded V_2O_5-WO_3/TiO_2 SCR catalyst at three different scales: transient runs were carried out over the catalyst crushed to powder and loaded in a microreactor with the purpose of studying the intrinsic kinetics of the NH_3-SCR reactions; a first scale-up was realized by conducting similar runs in an integral reactor,

using monolith core samples; finally, validation runs were performed over full-scale monoliths tested on a heavy-duty diesel engine test bench.

2.1. Microreactor experiments

In order to investigate the kinetics of the NH_3–NO/O_2 reacting system, experiments based on the transient response method (TRM) were run in the 175–450 °C temperature range: 160 mg of powdered catalyst obtained by grinding a commercial monolith catalyst to 140–200 mesh, diluted with 80 mg of quartz, were loaded into a flow-microreactor. The TRM runs were conducted feeding 1000 ppm of NO, 2% of O_2, 1% of H_2O at constant temperature and performing NH_3 step pulses (0 ppm → 1000 ppm → 0 ppm) with a GHSV of 210,000 h^{-1} or 90,000 h^{-1}. The temporal evolution of NH_3, NO, NO_2, N_2 and N_2O upon step variations of the NH_3 feed concentration was followed by a quadrupole mass spectrometer (Balzers QMS 200). Helium was used as inert carrier gas, so that the MS could detect nitrogen, which is the main SCR product, thus providing a complete description of the outlet gas composition and allowing the evaluation of overall N-balances. The influences of O_2 (2–6%, v/v) and H_2O (1–10%, v/v) feed concentrations were investigated by dedicated *T*-ramp experiments (*T*-range = 200–450 °C and heating rate = 10 K/min).

2.2. Monolith reactor experiments

Transient experiments were also run over extruded honeycomb catalyst samples of 22 mm and 44 mm length and 200 cpsi cell density. The reacting mixture was composed in this case by 900 ppm of NO, 10% of O_2 and 8% of water, while the NH_3 concentration varied between 720 ppm and 900 ppm. The outlet gas was analyzed using two different techniques: NH_3 was detected by microwave process analysis (Mipan) and NO_x by chemiluminescence using a modified low temperature NO_2 converter (CLD Ecophysics). The space velocity was set to 36,000 h^{-1} and 72,000 h^{-1} (referred to the overall monolith volume) with nitrogen as balance. Ammonia step pulses (0 ppm → 720 ppm or 900 ppm → 0 ppm) were carried out while continuously feeding NO.

2.3. Engine test bench experiments

Extruded monoliths with 300 cpsi, a wall thickness of 0.32 mm and a diameter of 144 mm were used in the runs on a heavy-duty diesel engine test bench. By varying the number of monoliths catalyst samples it was possible to test different catalyst volumes (251, 321 and 431). In the set of experiments presented in this paper, no oxidation catalyst was positioned upstream of the SCR catalysts; accordingly the NO_2 concentration was always negligible ($\leq$5%, v/v, of the total NO_x content). In all cases, urea was used to supply NH_3: an adequate residence time in the exhaust gas stream was allowed to secure its complete conversion to NH_3 before reaching the SCR catalyst.

A set of 100 different engine-operating points was measured and a sampling time of 2 Hz before and after the catalyst system was adopted to measure both temperatures and emissions using a chemiluminescence spectrometer for NO and NO_2 and a diode laser spectrometer for NH_3. A typical test bench experiment started when the engine run at constant load and speed. After a certain period, the urea dosing system introduced the reducing agent onto the catalyst, which resulted in an increase of the NO_x conversion after the SCR catalyst. After that NH_3-slip behind the catalyst could be measured. Typically, the experiment run until total NO_x conversion or steady state was established. Standard European test cycles (ESC and ETC), during which the catalyst outlet temperature varied between ca. 200 °C and 350 °C, were also performed at this scale.

3. Results and discussion

3.1. Kinetic runs

The complete set of the NH_3–NO/O_2 TRM microreactor runs over the powdered catalyst in the 175–450 °C temperature range was used to derive the intrinsic kinetics of the SCR process along the lines reported in [5]. Of specific interest herein are the transient experiments performed in the low *T*-region (175–250 °C) with 0–1000 ppm ammonia step feeds, while feeding 1000 ppm of NO in the presence of excess oxygen and water. In such experiments, a dynamic effect was clearly apparent during the fast decrease of the ammonia gaseous concentration associated with its shut off in the feed stream [5–7]. An example is shown in Fig. 1, where measured temporal evolutions of NH_3 (circles), NO (squares) and N_2 (triangles) outlet concentrations are plotted for a TRM experiment performed at 175 °C. At t = 1500 s, ammonia is removed from the feed stream and correspondingly the NO concentration trace decreases, goes through a minimum (at ca. t = 1850 s) and then begins to increase, recovering the inlet value when the reaction is depleted. This peculiar dynamic behaviour is confirmed by the symmetrical evolution of N_2 that indicates the occurrence of the SCR reaction.

Similar effects during ammonia shut off were always observed in transient experiments performed under equivalent conditions and $T < 250$ °C; comparable effects had been reported in the past also over different commercial SCR catalysts for stationary applications [8,9]: they are attributed to an inhibiting effect of excess NH_3, possibly caused by a competition between NO and ammonia in adsorbing onto the catalyst. Such inhibition effects are of limited interest for stationary applications of the SCR technology, but may play a considerable role in mobile applications, since they become more significant at low

temperatures and affect the dynamic response of the SCR systems. Accordingly, we address in the following the development and the validation of a SCR kinetic model suitable to describe the NH_3 inhibition effects at low temperatures. The implications of such effects on the catalytic mechanism of the SCR reaction over V-based catalysts are beyond the scope of this paper and will be discussed in a separate publication [7].

3.2. Derivation of the rate model

In order to fully describe the NH_3–NO/O_2 reacting system, NH_3 adsorption–desorption, NH_3 oxidation and SCR DeNOx reaction have to be considered, namely:

$$NH_3 \Leftrightarrow NH_3^* \quad (1)$$

$$4NH_3^* + 3O_2 \rightarrow 2N_2 + 6H_2O \quad (2)$$

$$4NH_3^* + 4NO + O_2 \rightarrow 4N_2 + 6H_2O \quad (3)$$

In previous work, in agreement with several literature and experimental indications [5,8–12], we adopted a standard Eley-Rideal rate law for the SCR reaction (3), thus assuming that the reaction occurred between adsorbed ammonia and gaseous (or weakly adsorbed) NO:

$$r_{NO} = k^{\circ}_{NO} \exp\left[-\frac{E_{NO}}{RT}\right] C_{NO}\theta_{NH_3} \quad (4)$$

The data fit obtained using Eley-Rideal kinetics was always satisfactory but for the NH_3 shut off transients at the lowest investigated temperatures [5], where the minima in the NO concentration observed at NH_3 shutdown and the corresponding maxima in the N_2 trace were not reproduced by the model, as evident in Fig. 1 (solid thin lines). This is not surprising since Eq. (4) does not consider the inhibiting effect of NH_3 on the SCR reaction, to which such a particular non-monotonic behaviour is ascribed. In order to take into account ammonia inhibition, we have developed and implemented an alternative rate expression, as summarized below.

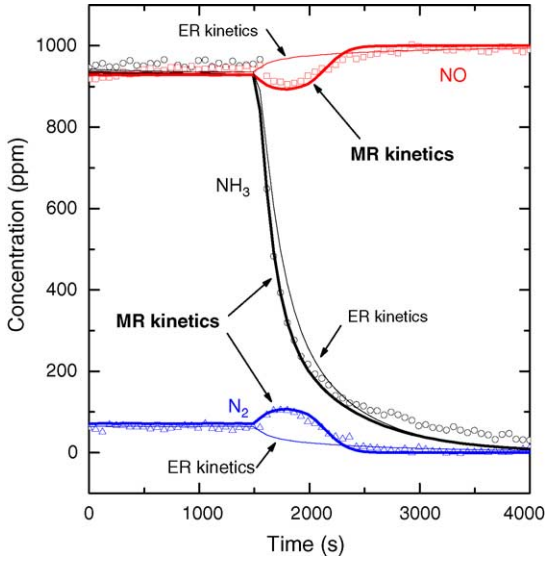

Fig. 1. $NH_3 + NO$ TRM run at 175 °C—GHSV = 210,000 h^{-1}, $C^{\circ}_{NO} = C^{\circ}_{NH_3} = 1000$ ppm. Symbols: outlet concentration of ammonia (circles), NO (squares) and N_2 (triangles). Solid thin lines: kinetic fit by ER rate expression (Eq. (4)). Solid thick lines: kinetic fit by modified redox rate expression (Eq. (12)).

In line with the derivations of SCR rate expressions for Mn_2O_3-WO_3/Al_2O_3 catalysts and for carbon supported V_2O_5 catalysts reported by Kapteijn et al. [13] and by Valdés-Solıs et al. [14], respectively, we assume that two different types of sites are present on the surface of the V_2O_5-WO_3/TiO_2 catalyst: one redox site for O_2 and NO adsorption/activation (S_1) and one acidic site for NH_3 adsorption (S_2). While for kinetic purposes this is not strictly relevant, we speculate that S_1-sites may be associated with Vanadyl species, whereas the S_2-sites are likely associated with other strongly acidic surface sites: it is well known in fact that NH_3 adsorption occurs also onto V-free WO_3/TiO_2 catalysts [15]. The possibility for NH_3 to adsorb onto sites other than the catalyst sites active for the DeNOx reaction, thus providing a "reservoir" for NH_3 storage/reaction, had been proposed in the past for $V/W/TiO_2$ SCR catalysts [10].

Starting from oxidized S_1-sites, we propose the following modified redox (MR) kinetic scheme:

(a) $S_1{=}O + NO \Leftrightarrow S_1{=}O[NO]$
(b) $S_2 + NH_3 \Leftrightarrow S_2[NH_3]$
(c) $S_1{=}O[NO] + S_2[NH_3] \rightarrow N_2 + H_2O + S_1{-}OH + S_2$
(d) $S_1{-}OH + 1/4O_2 \rightarrow S_1{=}O + (1/2)H_2O$

where reoxidation of reduced S_1-sites is represented by step (d).

In addition to steps (a)–(d), we assume also the following "NH_3 spill-over" step, involving adjacent S_1- and S_2-sites:

(e) $S_1{=}O + S_2[NH_3] \Leftrightarrow S_1{=}O[NH_3] + S_2$

The overall balances of S_1- and S_2-sites yield:

$$1 = \sigma_{free} + \sigma_{NO} + \sigma_{NH_3} + \sigma_{OH} \quad (5)$$

$$1 = \theta_{free} + \theta_{NH_3} \quad (6)$$

where the terms on the RHS of Eq. (5) represent the fractional coverages of $S_1{=}O$, $S_1{=}O[NO]$, $S_1{=}O[NH_3]$ and $S_1{-}OH$, respectively, while θ_{NH_3} in Eq. (6) indicates the fractional coverage of $S_2[NH_3]$.

We now express the rates of step (c), i.e. the surface reaction between adsorbed NO and NH_3, and of step (d), involving reoxidation of S_1-sites, as

$$r_{NO} = k_{NO}\sigma_{NO}\theta_{NH_3} \quad (7)$$

$$r_{reox} = k_{reox}C_{O_2}^{1/4}\sigma_{OH} \quad (8)$$

It is well known that reoxidation of the catalyst sites is the rate-controlling step in the standard SCR reaction at low

temperature. Accordingly, we impose that $r_{NO} = r_{reox}$, and obtain

$$\sigma_{OH} = \frac{k_{NO}\theta_{NH_3}}{k_{reox}C_{O_2}^{1/4}}\sigma_{NO} \quad (9)$$

Assuming quasi-equilibrium for steps (a) and (e), and taking advantage of Eq. (9), Eq. (5) becomes

$$1 = \sigma_{free}\left(1 + K_{NO}C_{NO} + K_{NH_3}\frac{\theta_{NH_3}}{1-\theta_{NH_3}} + \frac{k_{NO}K_{NO}C_{NO}\theta_{NH_3}}{k_{reox}C_{O_2}^{1/4}}\right) \quad (10)$$

Finally, incorporating Eq. (10) and further assuming negligible surface concentration of adsorbed NO, Eq. (7) becomes

$$r_{NO} = \frac{k_{NO}K_{NO}C_{NO}\theta_{NH_3}}{1 + K_{NH_3}\frac{\theta_{NH_3}}{1-\theta_{NH_3}} + \frac{k_{NO}K_{NO}C_{NO}\theta_{NH_3}}{k_{reox}C_{O_2}^{1/4}}} \quad (11)$$

In the limit of low NH_3 coverages, the redox rate Eq. (11) reduces to the familiar Eley-Rideal rate Eq. (4) successfully applied in the past to fit SCR kinetics in the medium–high temperature region [4]. Notably, Eq. (11) predicts no kinetic dependence on H_2O, in agreement with our experimental observations in the 1–10% (v/v) concentration range.

For the sake of simplicity, the following approximate form of Eq. (11), incorporating the kinetic dependence on O_2 into an empirical power-law term, was used for all the simulations herein reported:

$$r_{NO} = \frac{k'_{NO}O'\exp\left(-\frac{E_{NO}}{RT}\right)C_{NO}\theta_{NH_3}}{1 + K'_{NH_3}\frac{\theta_{NH_3}}{1-\theta_{NH_3}}}\left(\frac{p_{O_2}}{0.02}\right)^{\beta} \quad (12)$$

Eqs. (11) and (12) include functional dependences on the same variables: T, C_{NO}, θ_{NH_3} and C_{O_2}. Indeed, for all practical purposes they provided an equivalent fit of our kinetic runs. In the following we refer to Eq. (12) as the modified redox (MR) SCR rate law.

It is also worth emphasizing that adsorption/desorption equilibrium for NH_3 has not been assumed in the above derivation. The net rate of NH_3 reversible adsorption (step (b)) is herein written as

$$r_{NH_3} = k_{ads}C_{NH_3}(1 - \theta_{NH_3}) - k_{des}\theta_{NH_3} \quad (13)$$

In line with previous work [8–10,16], in Eq. (13) we further assume that k_{ads} is not activated, while account of catalyst heterogeneity, which is associated with a range of desorption activation energies [7,9], is included in k_{des} as follows:

$$k_{des} = k^{\circ}_{des}\exp\left(-\frac{E^{\circ}_{des}}{RT}(1 - \gamma\theta_{NH_3})\right) \quad (14)$$

At the highest investigated temperatures ammonia oxidation, reaction (3), was also observed; its rate is herein fitted by

$$r_{ox} = k^{\circ}_{ox}\exp\left(-\frac{E_{ox}}{RT}\right)\theta_{NH_3}\left(\frac{p_{O_2}}{0.02}\right)^{\beta} \quad (15)$$

3.3. Estimation of the intrinsic rate parameters and validation at the microreactor scale

The rate parameters in Eqs. (12)–(15) were estimated by global non-linear regression on the whole set of the NH_3–NO/O_2 TRM runs over the powdered catalyst in the 175–450 °C temperature range, adopting an isothermal PF model of the microreactor as detailed in [5]. An independent estimate of the NH_3 adsorption capacity Ω_{NH_3} was obtained from NH_3 adsorption isotherms at low temperature. Dedicated T-ramp experiments showed a negligible effect of the H_2O feed content above 1% (v/v). On the other hand, the effect of the O_2 feed concentration was not negligible, though small, and was nicely accommodated by rate Eqs. (12) and (15). The estimates of the rate parameters are listed in [6]: they were found consistent with other previous literature reports.

Fig. 1 compares the fit results obtained by using either the MR rate expression (Eq. (12)) (solid thick lines) or the ER kinetics (Eq. (4)) (solid thin lines): the redox kinetics can evidently account much better for the transient maxima–minima features of the experimental trace during the NH_3 shutdown phase. The same conclusion was reached comparing the data fits obtained with the two different rate expressions for several other transient experiments at low temperatures and at different space velocities [7]. The new rate law was also found superior to the modified Eley-Rideal kinetics proposed in Ref. [10] to account for the already mentioned "NH_3 reservoir" effect.

The MR kinetic model was further validated on a predictive basis by comparing its simulations with experimental data from microreactor runs consisting of high frequency NH_3 feed pulses in a stream of 1000 ppm of NO, 2% O_2 and 1% H_2O. A sample result is shown in Fig. 2: pulses, each consisting of 5 min with 1000 ppm of NH_3 feed and 5 min with no ammonia, were performed at 180 °C. The experimental signals (symbols in Fig. 2A or B) exhibit a characteristic transient behaviour: the greatest NO conversion is reached during each pulse after the NH_3 shut down, in agreement with the above mentioned ammonia inhibition effect. The same experiment was simulated using the isothermal PF model of the microreactor described in [5] using both the MR (Eq. (12)) and the ER (Eq. (4)) rate expressions. The simulation results are shown in Fig. 2A and B (solid lines), respectively.

Fig. 2 confirms that changing the DeNOx rate equation from the ER-based Eq. (4) to the new MR kinetic model (Eq. (12)) brings about a remarkable improvement in the description of fast SCR transients similar to those associated with the operation of SCR after-treatment devices for

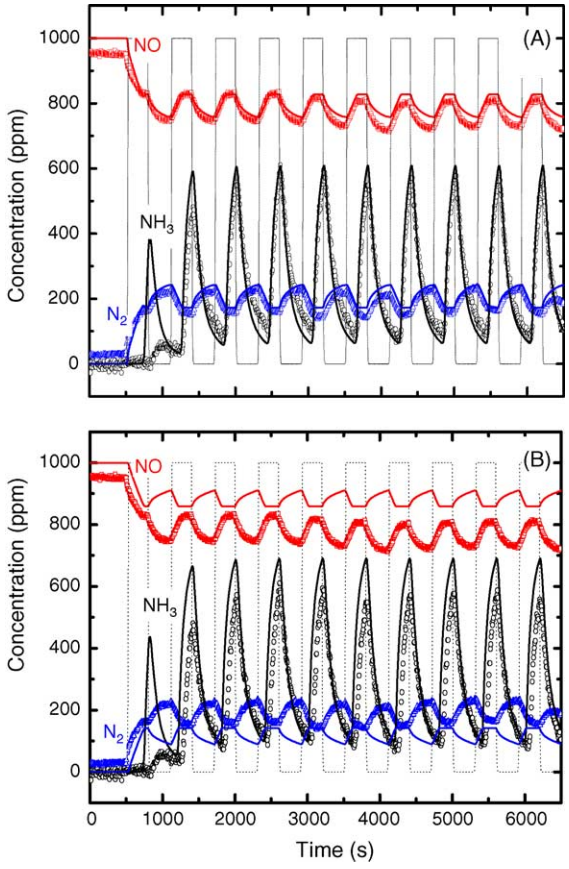

Fig. 2. Microreactor experiments with high frequency NH_3 feed pulses (1000 ppm) in flowing NO (1000 ppm) at 180 °C—GHSV = 90,000 h^{-1}. Symbols: outlet concentration of ammonia (circles), NO (squares) and N_2 (triangles). Dotted lines: inlet ammonia concentration. Solid lines: (A) simulation by MR rate law (Eq. (12)) and (B) simulation by ER rate law (Eq. (10)).

vehicles. Assuming a redox rather than an Eley-Rideal kinetic mechanism has also non-trivial implications concerning the catalytic mechanism of the SCR reactions, as further discussed in [7].

3.4. Dynamic model of SCR monolith reactors for automotive applications

In view of the use of extruded SCR monolith catalysts for vehicles, the 1D + 1D model herein presented accounts also for intraporous diffusion of the reacting species NH_3 and NO within the porous catalytic walls of the honeycomb matrix. Additional assumptions include negligible pressure drop and axial dispersion.

Unsteady mass and enthalpy balances for a single monolith channel are provided by the following equations, with symbols defined in the notation section:

gas phase:

$$\frac{\partial C_j}{\partial t} = -\frac{v}{L}\frac{\partial C_j}{\partial z} - \frac{4}{d_h}k_{mt,j}(C_j - C_j^w), \quad j = NH_3, NO \tag{16}$$

$$\frac{\partial T_g}{\partial t} = -\frac{v}{L}\frac{\partial T_g}{\partial z} - \frac{4}{d_h}h\frac{T_g - T_s}{\rho_g C_p} \tag{17}$$

solid phase:

$$0 = k_{mt,j}(C_j - C_j^w) + R_{eff,j}, \quad j = NH_3, NO \tag{18}$$

$$\frac{\partial T_s}{\partial t} = \frac{h(T_g - T_s) - \sum_{j=1}^{NCG}\Delta H_j R_{eff,j}}{\rho_s C_{p,s} S_w (1 + S_w/d_h)} \tag{19}$$

Gas–solid mass and heat transfer resistances are evaluated by analogy with the thermal Graetz-Nusselt problem for developing laminar flow in square ducts [17]. The strong intraphase diffusional limitations which can be associated with NH_3-SCR in extruded monolith catalysts are accounted for by the following equations for diffusion reaction of the reactants in the catalytic monolith walls,

$$0 = D_{eff,j}\frac{\partial^2 C_j^*}{\partial x^2} + S_w^2 R_j \quad j = NH_3, NO \tag{20}$$

$$R_{eff,j} = -\frac{D_{eff,j}}{S_w}\left.\frac{\partial C_j^*}{\partial x}\right|_w, \quad j = NH_3, NO \tag{21}$$

where R_j represents the volumetric intrinsic rate of formation of species j and S_w is the half-thickness of the monolith wall. Build up of reactants in the gas phase inside the catalyst pores is neglected, whereas accumulation/depletion of NH_3 adsorbed onto the catalyst surface, which is typically the controlling factor in the dynamics of SCR monolith reactors, is described by

$$\Omega_{NH_3}\frac{\partial \vartheta_{NH_3}}{\partial t} = R_{NH_3^*} \tag{22}$$

In addition to rate parameters and reaction conditions, the model requires the physico-chemical, geometrical and morphological (porosity, pore size distribution) characteristics of the monolith catalyst as input data. Effective diffusivities, $D_{eff,j}$, are then evaluated from the morphological data according to a modified Wakao-Smith random pore model, as specifically recommended for SCR monolithic catalysts [18].

3.5. Validation of the SCR monolith reactor model (laboratory scale)

Transient experiments with step pulses of NH_3 in a continuous flow of NO were also carried out over monolith catalyst samples. In such experiments the behaviour at low temperature was similar to the one observed over powdered catalyst: incremented NO_x conversions were detected at NH_3 shut down, in agreement with the ammonia inhibition effect discussed in the previous section. The results of such experiments were compared with model predictions generated by numerical solution of Eqs. (12)–(22). As in the case of the experiments over powdered catalyst (Fig. 2), the transient maxima–minima features of the experimental trace, as well as the increase of ammonia slip during

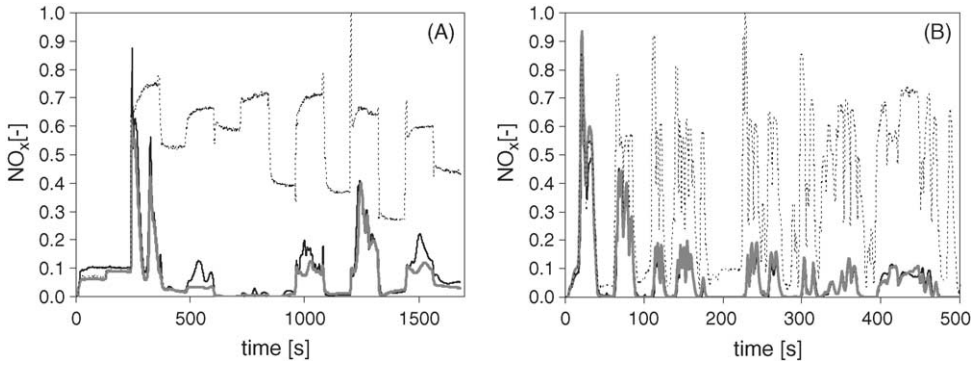

Fig. 3. Normalized NO_x concentration at SCR catalyst inlet and outlet of an ESC (A) and an ETC (B) test cycle. Dotted black lines, inlet values; solid black lines, outlet measurement; grey lines, outlet simulation.

successive pulses, were well simulated by the model including the MR rate expression (Eq. (12)). On the contrary, the use of the Eley-Rideal rate expression (Eq. (4)), also in the case of monolith catalysts, inverted the phase of the simulated NO signal, just as shown in Fig. 2B.

3.6. Validation of the SCR monolith reactor model (full scale)

As discussed in Section 2, both steady state and transient experimental runs were systematically carried out over a full-scale catalytic converter with real engine exhaust gas in order to evaluate the goodness of the predictions of the SCR monolith reactor model. Validation maps were generated using the steady state measured engine-operating points. In this case, the deviation between simulated NO_x conversion and experimental data was typically below 4% [6]. Transient ESC and ETC runs were then performed over the same system. The comparison between measurement and simulation for the NO_x concentrations downstream of the catalyst reveals an excellent correlation, as can be seen by Fig. 3A (ESC) and B (first 500 s of ETC). NO_x concentrations have been normalized by the maximum inlet value during the test cycles. The overall DeNOx efficiency within the ESC or ETC test cycle could be predicted with an error of 3–4%. These results confirm that the model, including the MR rate Eq. (12), is able to predict accurately the dynamic behaviour of SCR monolith catalysts under fast transient conditions. Using the Eley-Rideal rate law (Eq. (4)) resulted in a significantly less accurate prediction of the NO_x conversion during the fast transient parts of the test cycles.

4. Conclusions

Concepts and methods applied in the past to develop engineering models of the NH_3-SCR DeNOx process for power stations can be used successfully for mobile applications of the SCR technology as well. However, transient operation of SCR devices for vehicles is more demanding, requiring an improved adherence of the assumed kinetic description to the real catalytic mechanism for optimal results. In this respect, the findings herein reported have pointed out that this is indeed critical for accurate simulation of SCR after-treatment systems for mobile applications: rate Eq. (12), accounting for NH_3 inhibition effects at low temperatures, yields substantially improved agreement with fast transients of the standard NH_3-SCR reaction with NO as compared to previous traditional or modified Eley-Rideal approaches. Furthermore, the identification of an optimal NH_3 surface coverage, as predicted by Eq. (12), may be an important factor in the design of ammonia/urea dosage strategies. Based on the present results, a specific investigation of the mechanistic phenomena in the NH_3-SCR over V-based catalysts at low temperatures ($\leq$250 °C) seems of both practical and fundamental interest.

This paper also illustrates a fully transient 1D + 1D model of SCR monolith reactors for automotive applications, which has been successfully validated against data at different scales: it is now being used as a powerful tool for development and design of after-treatment devices for vehicles.

Acknowledgment

Useful discussions with Professor Pio Forzatti are gratefully acknowledged.

References

[1] ACEA Final Report on Selective Catalytic Reduction, June 2003, http://europa.eu.int/comm/enterprise/automotive/mveg_meetings/meeting94/scr_paper_final.pdf.
[2] P. Forzatti, L. Lietti, E. Tronconi, Nitrogen oxides removal-E (Industrial), in: I.T. Horvath (Ed.), Encyclopedia of catalysis, J. Wiley, New York, 2002.
[3] A. Kato, S. Matsuda, T. Kamo, F. Nakajima, H. Kuroda, T. Narita, J. Phys. Chem. 85 (1981) 4099.
[4] E. Tronconi, A. Cavanna, P. Forzatti, Ind. Eng. Chem. Res. 37 (1998) 2341.

[5] C. Ciardelli, I. Nova, E. Tronconi, B. Konrad, D. Chatterjee, K. Ecke, M. Weibel, Chem. Eng. Sci. 59 (2004) 5301.
[6] D. Chatterjee, T. Burkhardt, B. Bandl-Konrad, T. Braun, E. Tronconi, I. Nova, C. Ciardelli, SAE Paper 2005-01-965 (2005).
[7] I. Nova, C. Ciardelli, E. Tronconi, D. Chatterjee, B. Bandl-Konrad, in preparation.
[8] I. Nova, L. Lietti, E. Tronconi, P. Forzatti, Catal. Today 60 (2000) 73.
[9] I. Nova, L. Lietti, E. Tronconi, P. Forzatti, Chem. Eng. Sci. 56 (2001) 1229.
[10] L. Lietti, I. Nova, S. Camurri, E. Tronconi, P. Forzatti, AIChE J. 43 (1997) 2559.
[11] N.-Y. Topsoe, J.A. Dumesic, H. Topsoe, J. Catal. 151 (1995) 241.
[12] U.S. Ozkan, Y. Cai, M.W. Kumthekar, J. Phys. Chem. 99 (1995) 2363.
[13] F. Kapteijn, L. Singoredjo, N.J.J. Dekker, J.A. Moulijn, Ind. Eng. Chem. Res. 32 (1993) 445.
[14] T. Valdés-Solıs, G. Marban, A.B. Fuertes, Ind. Eng. Chem. Res. 43 (2004) 2349.
[15] L. Lietti, J.L. Alemany, P. Forzatti, G. Busca, G. Ramis, E. Giamello, F. Bregani, Catal. Today 29 (1996) 143.
[16] G. Busca, L. Lietti, G. Ramis, F. Berti, Appl. Catal. B 18 (1998) 1.
[17] E. Tronconi, P. Forzatti, AIChE J. 38 (1992) 201.
[18] J.W. Beekman, Ind. Eng. Chem. Res. 30 (1991) 428.